Proceedings of the
International Conference on Mechanical Engineering and Renewable Energy 2013
(ICMERE2013) 1 - 3 May 2014, Chittagong, Bangladesh

ICMERE2013-PI-040

THERMAL ANALYSES OF NANO AND MICRO SATELLITES POINTING TO THE EARTH WITH DEPLOYABLE SOLAR PANEL BY SMALL NUMBER OF NODES

Tilok Kumar Das[1*], Tsuyoshi Totani[2], Masashi Wakita[2] and Harunori Nagata[2]

[1*]Graduate school of Engineering, Hokkaido University, Japan
[2] Faculty of Engineering, Hokkaido University, Japan
*tilok_cuet@yahoo.com, tota@eng.hokudai.ac.jp, m-wakita@eng.hokudai.ac.jp,
nagata@eng.hokudai.ac.jp

Abstract*- This paper represents thermal analysis of nano and micro satellites of 50 cm cube pointing to the Earth with deployable solar panel on sun-synchronous and circular orbits at altitude of 500 km using few nodal analyses. Satellites of smaller size nano and micro satellites such as STARS, RISESAT are launching recently. Projected area of satellite with and without deployable solar panel at LTDN 10 is shown in order to understand comparative advantages of satellite with deployable solar panel over without deployable solar panel. In addition power generated by Satellite with deployable solar panel considering 5 surfaces of cube part and top sides of deployable solar panel covered completely that means removing solar cell from earth pointing surfaces and bottom sides respectively are carried out for LTDN from 6 to 12 and highest average generated power 149.47 W and 132.65 W for LTDN 11 in worst hot case and worst cold case respectively. Numbers of combinations of optical properties of micro and nano satellites with deployable solar panel for all LTDN are carried out which is higher in the case of LTDN without shadow region than with shadow region.*

Keywords: Thermal design, Micro satellites, Nano satellites, Sun-synchronous orbit.

1. INTRODUCTION

Nano and Micro satellite are very popular now-a-days among different kinds of satellites that are sending into space. There are many reasons why it is getting wide acceptance for the field of space systems. First of all it is cheaper in compare with large and medium satellites and fabrication time can be abridged like one and half year after receiving contract. New technologies can be implemented as an updating satellite system and its functioning. Moreover it can be used for excellent teaching material to realize how its work in space for educational institution. Applications of nano and micro satellites is not only limited in teaching tools for students but also we can use these kinds of satellites for many business purposes such as observing disasters, flood or agricultural purposes. Micro and nano satellite does not have any propulsion system to shift from orbit of one local time of descending node to orbit of another local time of descending node with the help of data handling system controlled by server from ground station. There is a possibility to change local time of descending node of micro and nano satellites due to oblateness of the Earth. It is important to have a good thermal design of micro and nano satellites for working it all components properly. In order to prepare a micro and nano satellites within very short time, we need to establish guideline such as maximum power generation capacity during moving in different local time of descending node. The combination of optical properties on structures and components to keep the temperature within the design temperature range are clarified using one nodal, two nodal and multi-nodal analyses in case of satellite without deployable solar panel by Totani et. al [1][2]. Relative advantages of micro and nano satellite with deployable solar panel over body mounted solar panel for producing greater energy are carried out in this paper. Combination of Optical properties such as absorptivity and emissivity of micro and nano satellite are shown in this paper.

2. METHOD OF ANALYSIS

2.1 Projected Area of Satellite

Details description about projected area of Micro and Nano satellite of cube shape without deployable solar panel or body mounted solar panel has done for local of descending node from 6 to 12 at same altitude of 500 km with respect to Sun in winter solstice by Totani et al. [3]. Figure 1 and Figure 2 shows satellite with and without deployable solar panel respectively. Analysis over satellite with deployable solar panel is carried out in this paper specially. Figure 6 presents the comparison of projected area of satellite with and without deployable solar panel for local time of descending node at 10 of 500 km altitude with respect to Sun in winter solstice without considering shadow region of Earth. Because in the case that satellite goes inside shadow region of Earth, there will be no projected area with respect to the Sun. Unit length is considered for length of each side of satellite. Projected area for satellite with deployable solar panel is the summation of main part of satellite, top side and bottom side of deployable solar panel. The main purpose of using deployable solar panel in satellite is to increase the projected area with respect to Sun during moving in orbit for generating large amount of power than satellite without deployable solar panel.

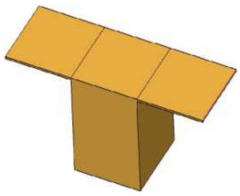

Fig.1: Satellite with deployable solar panel

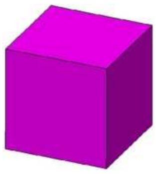

Fig.2: Satellite without deployable solar panel

2.2 Power Generation

It is very important to know that how much power can be generated by solar cell mounted on different surfaces. Maximum load can be installed inside satellite depends on power generation capability by solar cell. It is possible to determine filling factor for satellite by this analysis that means how much surface will be covered of total surfaces area of satellite in order to satisfy power demand by load given inside of satellite. Figure 3 shows schematic diagram considering shadow and sunshine region of satellite travelling on orbit. Depending on altitude and local time of descending node satellites does not enter into the shadow region. For instance, at 500 km altitude a satellite does not enter into shadow region of earth for local time of descending node 6 and 7 on sun-synchronous orbit in winter solstice. Considering satellite start moving from at the entrance of shadow region ($t = t_s$) and satellite exit shadow region when $t = t_e$. It keeps moving in sunshine region for a period, say $t = t_0$ and finally reach in initial position at $t = t_f$. As a result, the relation among all times from start to end is given below

$$t_s < t_e < t_0 < t_f$$

Electricity is generated by solar cell only in the sunshine region. General equation is used for calculating power generation for one rotation in orbit by solar cell is shown below.

$$P_{gen} = \int_{t_s}^{t_f} \rho_c n_c G_s \left(A_p + aF_a l^2\right) dt \quad \dots \dots (1)$$

Different conditions can be considered for generating power such as solar cell mounted on

a) all the surfaces covered with solar cell,
b) 6 surfaces and Top sides covered with solar cell
c) 5 surfaces and Top sides that mean removing solar cell from earth pointing surface and bottom surfaces.

In this paper case (c) result is considered, because in practical case there is no solar cell on earth pointing surface due separation system, telescope are mounted in this surface. Filling factor is equal 1 that means 5 surfaces and top sides of deployable solar panel covered with solar cell completely. Top surfaces do not receive any albedo from earth because there is a surface always

Table 1: Angle of shadow region for 500 km altitude

LTDN	Gamma1	Gamma2	Gamma
6	0	0	0
7	0	0	0
8	75.98	168.99	93.01
9	56.96	174.25	117.29
10	48.61	177.16	128.55
11	45.33	179.32	133.99
12	45.28	181.25	135.97

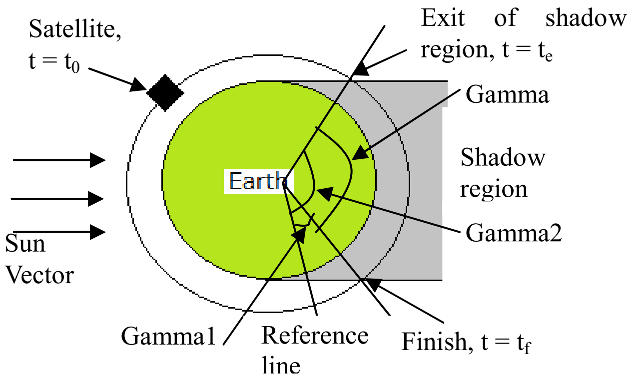

Fig.3: Satellite moving in orbit

Table 2: Worst hot case and worst cold case

Parameter	Worst cold case	Worst hot case
Solar contact, W/m^2	1309	1414
Earth infrared radiation,W/m^2	189	261
Albedo Factor	0.2	0.4
Initial temperature, K	10	25
Initial position for calculation	Entrance of eclipse	Exit of eclipse

pointing to the earth. Table 1 shows angle of shadow region for local time of descending from 6 to 12 at 500 km altitude. Gamma 1 represents angle at the entrance of shadow region and gamma 2 exit of shadow region angle and finally gamma indicates angle of shadow region for different LTDN which is equal the difference between gamma2 and gamma1. Table 2 shows information about worst hot and cold case is considered in this paper. Both worst hot and cold case separate results were obtained from this analysis. In this case 8000 grid points are considered to calculate generated power by satellite.

2.3 Energy Equation

Table 3 and Table 4 show information about satellite model defined for this analysis. Figure 4 shows input and output heat is considered for satellite with deployable solar panel model to analysis the optical properties in this paper. Basic schematic diagram and energy equations for satellite without deployable solar panel were presented by Totani et. al [3]. The basic difference in schematic diagram of satellite with or without deployable solar panel is additional heat exchange need to consider such as reflection and radiation from main part of satellite with deployable solar panel. In other words heat transfer from main part of satellite to deployable solar and reverse depends on temperature gradient. Equation 2 and 3 for main part of satellite and deployable solar panel include radiation and reflection terms that are considered respectively. In the case of reflection, diffusive reflection is assumed. Equations for main part of satellite and deployable solar panel in this analysis are given separately.

Table 3: Shape, orbit, attitude, and setting method of solar panel of satellites analyzed in this paper.

Shape	Cube with deployable solar panel
Orbit	Sun-synchronous and circular orbit
Attitude	Earth-pointing
Altitude	500 km
Inclination	97.4 degree
Setting method of solar panel	Body mounted and deployable solar panel.
Allowable temperature range for MPS.	0~40 degree Celsius
Allowable temperature range for DSP.	-145~ 65 degree Celsius

Table 4: Size, mass, heat capacity of satellites

Mass of MPS, m_1 [kg]	50
Mass of DSP, m_2 [kg]	2
Size l^3 [cm^3]	50×50×50
Thickness of DSP plate, t [mm]	1.5
Heat capacity of MPS, m_1c [J/K]	36000
Heat capacity of DSP, m_2c [J/K]	1440

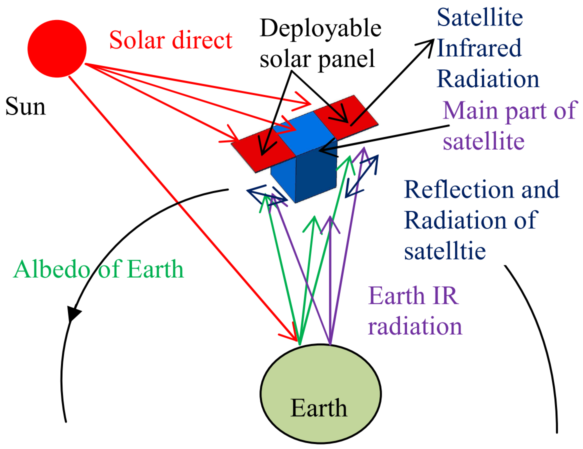

Fig.4: Schematic of heat input and output from satellite

Equations for main part of satellite:

$$Q_{ds} + Q_{alb\text{-}fearth} + Q_{IR} + Q_{reflin\text{-}fdsp} + Q_{radin\text{-}fdsp} + Q_{com} - P_{gen1} - Q_{radiation\text{-}fmps} = m_{mps} C_{mps} \frac{dT_{mps}}{dt} \ \ldots\ldots\ldots (2)$$

Where, $Q_{ds} = \alpha_{mps}\, G_s\, A_{pmps}$

$Q_{alb\text{-}fearth} = \alpha_{mps}\, G_s\, a\, (F_{n\, s-e}\, l^2 + 4\, F_{p\, s-e}\, l^2)\cos\theta$

$Q_{IR} = \varepsilon_{mps}\, q_{IR}\, (F_{n\, s-e}\, l^2 + 4\, F_{p\, s-e}\, l^2)$

$Q_{reflin\text{-}fdsp} = F_{fdsp\text{–}mps}\, (\varepsilon_{mps}\, Q_{IR} + \alpha_{mps}\, Q_{alb\text{-}fearth} + \alpha_{mps}\, Q_{ds})_{fdsp}$ (considering diffusive reflection)

$(Q_{IR})_{fdsp} = 2\,(1 - \varepsilon_{bsdsp})\, q_{IR}\, A_{bsdsp}\, F_{ndsp-e}$

$(Q_{alb\text{-}fearth})_{fdsp} = 2\,(1 - \alpha_{bsdsp})\, G_s\, a\, A_{bsdsp}\, F_{ndsp-e}\cos\theta$

$(Q_{ds})_{fdsp} = (1 - \alpha_{bsdsp}) G_s\, A_{pbsdsp}$

$Q_{radin\text{-}fdsp} = 2\, \varepsilon_{mps}\, F_{fdsp\text{–}mps}\, \varepsilon_{bsdsp}\, A_{bsdsp}\, \sigma\, T_{dsp}^{\ 4}$

$Q_{radiation\text{-}fmps} = \varepsilon_{mps}\, 6\, l^2 \sigma\, T_{mps}^{\ 4}$

Equations for deployable solar panel of satellite:

$$Q_{ds} + Q_{alb\text{-}fearth} + Q_{IR} + Q_{reflin\text{-}fmps} + Q_{radin\text{-}fmps} - P_{gen2} - Q_{radiation\text{-}fdsp} + Q_{shnt} = m_{dsp} C_{dsp} \frac{dT_{dsp}}{dt} \ \ldots\ldots\ldots (3)$$

Where, $Q_{ds} = \alpha_{tsdsp}\, G_s\, A_{ptsdsp} + \alpha_{bsdsp}\, G_s\, A_{pbsdsp}$

$Q_{alb\text{-}fearth} = \alpha_{bsdsp}\, G_s\, a\, (2\, A_{bsdsp}\, F_{ndsp-e} + 6\, F_{pdsp-e}\, l\, t_c)\cos\theta$

$Q_{IR} = \varepsilon_{bsdsp}\, q_{IR}\, (2\, A_{bsdsp}\, F_{ndsp-e} + 6\, F_{pdsp-e}\, l\, t_c)$

$Q_{reflin\text{-}fmps} = F_{fmps\text{–}dsp}\, (\varepsilon_{bsdsp}\, Q_{IR} + \alpha_{bsdsp}\, Q_{alb\text{-}fearth} + \alpha_{bsdsp}\, Q_{ds})_{fmps}$ (considering diffusive reflection)

$(Q_{IR})_{fmps} = 2\,(1 - \varepsilon_{mps})\, q_{IR}\, F_{p\, s-e}\, l^2$

$(Q_{alb\text{-}fearth})_{fmps} = 2\,(1 - \alpha_{mps})\, G_s\, a\, F_{p\, s-e}\, l^2 \cos\theta$

$(Q_{ds})_{fmps} = (1 - \alpha_{mps})\, G_s\, A_{pmps1}$

$Q_{radin\text{-}fmps} = 2\, \varepsilon_{bsdsp}\, F_{mps\text{–}fdps}\, \varepsilon_{mps}\, l^2 \sigma\, T_{mps}^{\ 4}$

$Q_{radiation\text{-}fdsp} = 6\, \varepsilon_{bsdsp}\, l\, t_c\, \sigma\, T_{dsp}^{\ 4} + (2\, \varepsilon_{tsdsp}\, A_{tsdsp} + 2\, \varepsilon_{bsdsp}\, A_{bsdsp})\, \sigma\, T_{dsp}^{\ 4}$

2.4 Optical Properties

In order to determine optical properties of satellite, two nodal analyses are considered that means one node in deployable solar panel and another one node in main part of satellite. Whole orbit is divided into 8000 grid point in order to calculate optical properties identifying entrance and exit of shadow region.

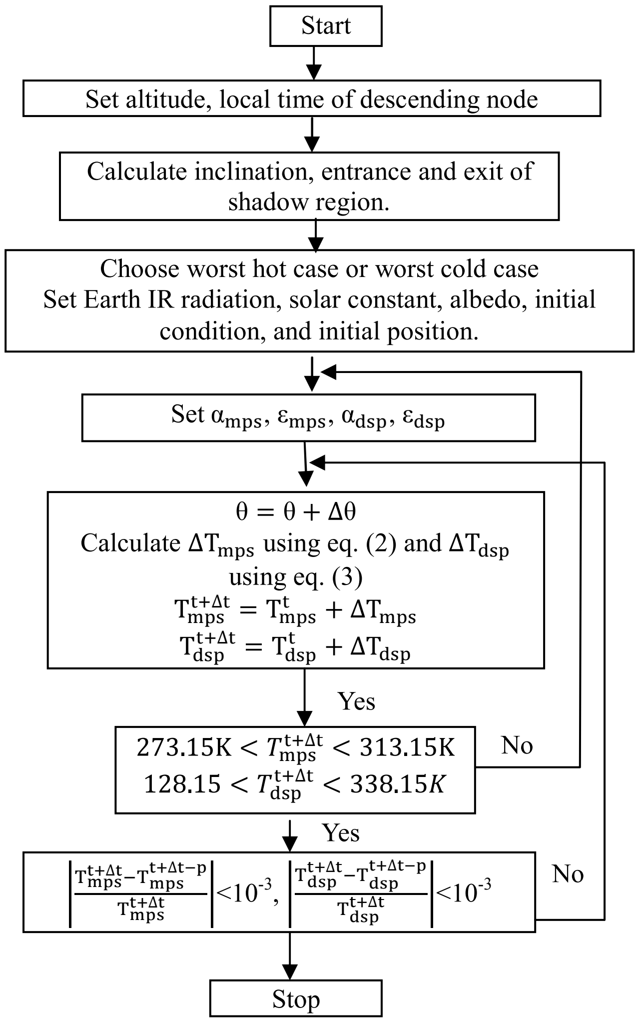

Fig.5: Flow chart of optical properties calculation

Table 5: Specifications of analyses program

Programming Language	Fortran 90
Compiler	g95
Variable type	Double precision

It is difficult to fix specific heat of main part of satellite and deployable solar panel. The specific heat is considered 720 J/(kg K) in such a way that temperatures of components changes easily. Temperature is considered constant for whole main part of satellite. This value corresponds to 80% of the specific heat of aluminum alloy A5052, 900 J/(kg K) [1]. Again two deployable solar panels are in same temperature during obtaining optical properties from analyses. Figure 5 shows flow chart for two nodal analyses to obtain optical properties in this program. Maximum and minimum average power consumption is 100W and 40W respectively for this analysis. The interval for optical properties both absorptivity and emissivity of deployable solar panel of satellite is 0.1.

3. RESULTS AND DISCUSSION

Figure 6 shows projected area calculated for satellite with and without deployable solar panel for local time of descending node 10. It presents projected area for satellite with deployable solar panel larger than satellite without deployable solar panel of same size. It is obvious that minimum projected area of satellite with deployable solar panel is same as satellite with body mounted solar panel. But maximum projected area is large for long period in the same orbit in the case of satellite with deployable solar panel. Increasing the amount of projected area is important from view point generating large amount power for components installed inside satellite. The more generated power the more components can be installed for obtaining information from satellite. In this case projected area for LTDN 10 is compared to show advantage from deployable solar panel. Figure 7 shows average power that can be generated on orbit. From analysis it is observed that power generation by satellite increase with the increase of LTDN. But power generation was reduced at LTDN 8 as shown in Figure 7, because it entered into shadow region at LTDN 8 of 500 km altitude. Again power generation is increased by satellite due to increase in projected area from LTDN 6 to 12. It is possible to obtain maximum power generation at LTDN 11 considering shadow region. Projected area of satellite with deployable solar panel at LTDN 12 was increased but at same time shadow region also was increased. From Table 6 show acme power obtained from analysis at LTDN 11 and 12 with angle of shadow region. It is observed that acme power for LTDN 12 higher than LTDN11. As it is mentioned in Table 6 angle of shadow region for LTDN 11 and 12 are 133.99 and 135.97 degree respectively at 500 km altitude. Therefore, maximum amount of average power generation could not be obtained at local time of descending node 12. From Figure 8 and 9 shows power generation by satellite at each point in orbit. It is clear the reason why power generation dropped in case of local time of descending node 8. It can be seen from figure that there is a continuous power generation by satellite for LTDN 7 because there was no shadow region. Satellite passes both shadow and sun shine region in the case of LTDN 8. Similarly from LTDN 9 to12, there is no power generation in the shadow region. From above

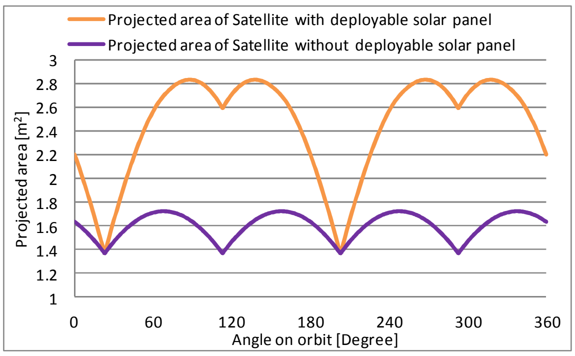

Fig.6: Comparison of projected area of satellite with and without deployable solar panel at LTDN 10

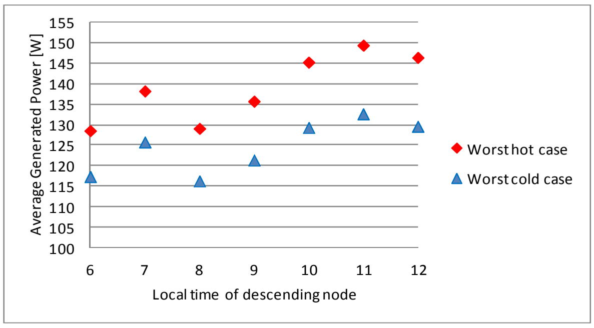

Fig.7: Average generated power in different LTDN

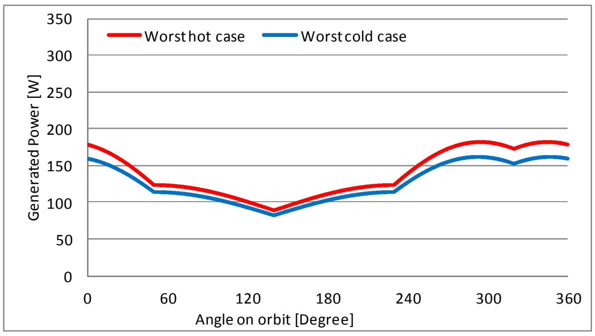

Fig.8: Power generated by solar cell at LTDN 7

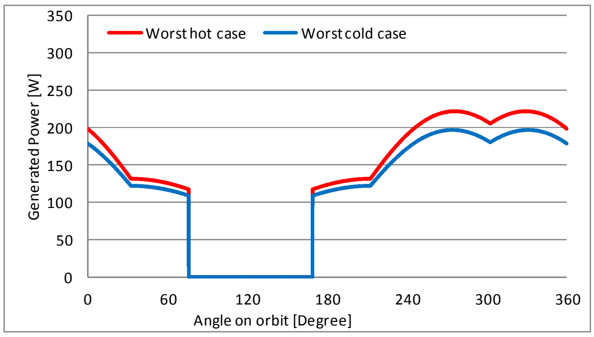

Fig.9: Power generated by solar cell at LTDN 8

Table 6: Peak power with local time of descending node

LTDN	Peak Power [W]		Angle of shadow region [Degree]
	Worst hot case	Worst cold case	
11	328.39	287.06	133.99
12	338.56	295.52	135.97

circumstances, it can concluded that for generating maximum power satellite must placed in the higher number of local time of descending such as 10, 11 and12. From Figure 10, 11 show the combinations of optical properties for local time of descending node at 8, 11 respectively. Shunt is placed on deployable solar panel in this analysis and numbers of combinations are obtained in different local time of descending node at the altitude of 500 km. The numbers of combination are decreasing with increase of LTDN. The reason why it was happen that projected area is increasing with increase of LTDN and there was no shadow region for LTDN 6 and 7 at 500 km altitude but satellites enter into shadow region from local time of descending node 8. At that situation numbers of combination of optical properties were decreased significantly. The numbers of combination of optical properties were maximum for local time of descending node of 6 and 7 that means when there is no shadow region. Later with the increase of LTDN and angle of shadow region, numbers of combination of optical properties reduced. These combinations of optical properties of main part of satellite are not independent itself but it also depends on the combination of optical properties of deployable solar panel because there was heat transfer by reflection and radiation in order to satisfy allowable temperature range 0 to 40 degree Celsius for main part of satellite and -145 to 65 degree Celsius for deployable solar panel. This numbers of combination of optical properties could be increased if change in optical properties of satellite of deployable solar panel decreased from 0.1 to less for instance 0.01. Figure 12 show temperature history corresponding two specific combination optical properties where one satisfy allowable temperature range and another does not satisfy allowable temperature range of satellite both main part of satellite and deployable solar panel. In case of absorptivity 0.66 and emissivity 0.48 temperature of history does not exceed the range of 0 to 40 degree Celsius for main part of satellite that combination of

Table 7: Relation of LTDN with Combination of Optical properties

LTDN	Number of Combination of optical properties in main part of satellite
6	1147
7	1257
8	412
9	169
10	95
11	57
12	42

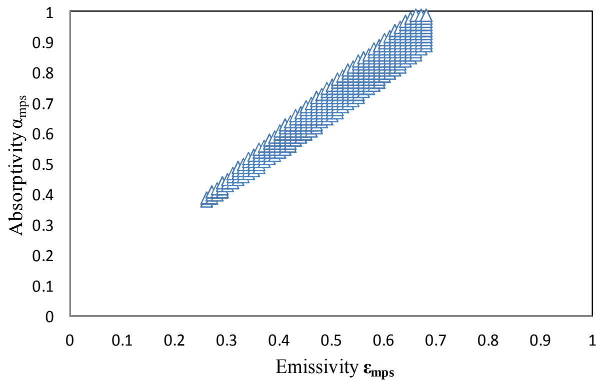

Fig.10: Combinations of optical properties at LTDN 8

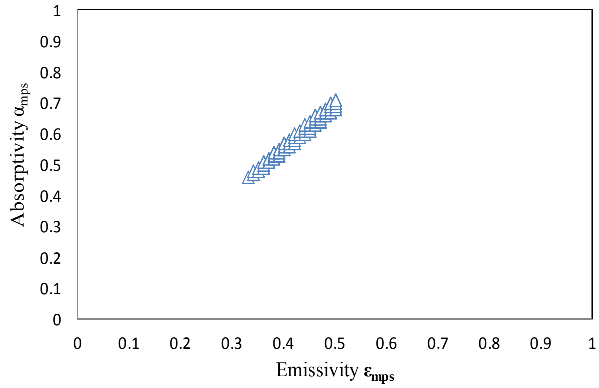

Fig.11: Combinations of optical properties at LTDN 11

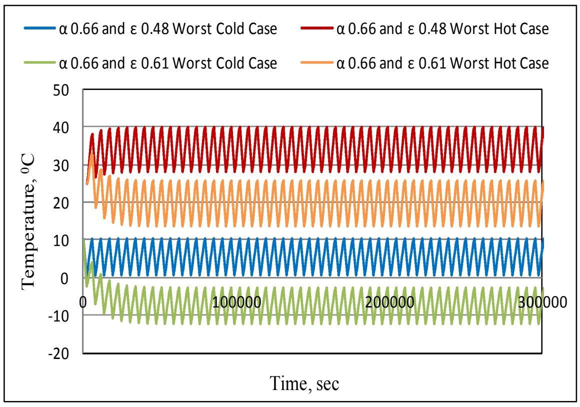

Fig.12: Temperature history of main part of satellite at LTDN 11 for different combination of optical properties

optical properties was obtained from two nodal analysis of satellite with deployable solar panel. On the other hand in case of absorptivity 0.66 and emissivity 0.61 temperature history of satellite of main part of satellite does not satisfy temperature in both worst hot and cold case. Although worst hot case keep inside temperature range but temperature goes below 0 degree Celsius in case of worst cold case. It is important to choose suitable optical properties for satellite in order to keep temperature of satellites in allowable temperature range.

4. CONCLUSION

Projected area is compared with and without deployable solar panel at local time of descending node

10 in this paper. Average generated power of satellite with deployable solar panel is shown from LTDN 6 to 12 considering a satellite each side length of 50 cm in order to understand maximum power that satellite can provide assuming surfaces covered with solar cell completely on sun-synchronous and circular orbit at the altitude of 500 km. Highest average generated power 149.47 W and 132.65 W was obtained for LTDN 11 in worst hot case and worst cold case respectively from all LTDN from 6 to 12. Maximum number of combinations of optical properties was obtained for local time of descending node 6 and 7 that means when there is no shadow region. Two nodal analyses are considered for determining optical properties where main part of satellite is one node and another node is deployable solar panel. Generated power for different LTDN has a good image for future satellite load installment.

5. ACKOWLEDGEMENT

This research is granted by the Japan Society for the promotion of Science (JSPS) through the “Funding Program for World-Leading innovative R&D on Science and Technology (First Program),” initiated by the council for Science and Technology Policy (CSTP).

6. REFERENCES

[1] T. Totani, H. Ogawa, Ryota Inoue, T. K. Das, M. Wakita, H. Nagata, “Proposal of Procedure of Thermal design on Micro and Nano satellites point to Earth” *43rd International Conference on Environmental Systems*, AIAA 2013-3490, 14-18 July 2013, Vail, CO.

[2] R. Inoue, T. Totani, H. Ogawa, M. Wakita, H. Nagata, “Thermal analyses and guideline of Nano and Micro satellites on Sun-synchronous orbits” *4th Nano Satellite Symposium*, October 10-13, 2012, Nagoya, Japan.

[3] T. Totani, H. Ogawa, R. Inoue, M. Wakita, H. Nagata, “One Nodal Thermal analysis for Nano and Micro satellites on Sun-synchronous orbits” *Trans. JSASS Aerospace Tech. Japan*, Vol. 11, pp. 71-78, 2013.

[4] Japan Aluminum Association, Characteristics Data base of Aluminum Materials [online database], URL: http://metal.matdb.jp/JAA-DB/ [cited 4 March2013]

[5] D. G. Gilmore “Spacecraft Thermal control Handbook” 2nd Edition, Vol. 1, the aerospace Press, EI Segundo, 2002, Appendix A

7. NOMENCLATURE

Symbol	Meaning	Unit
a	Albedo factor	
A_p	Projected area	
A_{pmps}	Projected area of MPS	(m^2)
A_{pbsdsp}	Projected area of bottom side of DSP	(m^2)
A_{ptsdsp}	Projected area of top side of DSP	(m^2)
A_{tsdsp}	A top surface area of DSP	(m^2)
A_{bsdsp}	A bottom surface area of DSP	(m^2)
A_{pmps1}	Projected area of MPS consider the surface close to DSP	(m^2)
C_{mps}	Specific Heat of MPS	(J/kg/K)
C_{dsp}	Specific Heat of DSP	(J/kg/K)
$F_{n\,s-e}$	View factor from the earth pointing surface of MPS to the earth	
$F_{p\,s-e}$	View factor from the surface parallel to the position vector of MPS to the earth.	
F_{ndsp-e}	View factor from the lower side DSP to the earth	
F_{pdsp-e}	View factor from the surface parallel to the position vector of DSP to the earth.	
$F_{fdps-mps}$	View factor from DSP to MPS	
$F_{fmps-dsp}$	View factor from MPS to DSP	
G_s	Solar constant	(W/ m^2)
l	Length of side of MPS	(m)
m_{mps}	Mass of MPS	(kg)
m_{dsp}	Mass of DSP	(kg)
P_{gen1}	Power generated by MPS	(W)
P_{gen2}	Power generated by DSP	(W)
q_{IR}	Earth Infrared Radiation	(W/ m^2)
Q_{ds}	Solar direct	(W)
Q_{IR}	Heat input by Earth Infrared Radiation	(W)
Q_{com}	Heat generated from component	(W)
$Q_{alb\text{-}fearth}$	Heat input by Earth albedo	(W)
$Q_{reflin\text{-}fdsp}$	Reflected energy input from DSP to MPS	(W)
$Q_{reflin\text{-}fdsp}$	Reflected energy input from DSP to the MPS	(W)
$Q_{radin\text{-}fmps}$	Radiation absorbed by DSP from MPS	(W)
$Q_{radin\text{-}fdsp}$	Radiation absorbed by MPS from DSP	(W)
$Q_{radiation\text{-}fmps}$	Radiation from MPS	(W)
$Q_{radiation\text{-}fdsp}$	Radiation from DSP	(W)
Q_{shnt}	Heat produced due to shunt	(W)
$(Q_{IR})_{fdsp}$	Reflected energy by Earth IR radiation from DSP to MPS	(W)
$(Q_{alb\text{-}fearth})_{fdsp}$	Reflected energy by albedo of earth from DSP to MPS	(W)
$(Q_{ds})_{fdsp}$	Reflected energy by solar direct from DSP to MPS	(W)
$(Q_{IR})_{fmps}$	Reflected energy by Earth IR radiation from MPS to DSP	(W)
$(Q_{alb\text{-}fearth})_{fmps}$	Reflected energy by albedo of earth from MPS to DSP	(W)
$(Q_{ds})_{fmps}$	Reflected energy by solar direct from DSP to MPS	(W)
T_{dsp}	Temperature of DSP	(K)
T_{mps}	Temperature of MPS	(K)
t	Time	sec
t_c	Thickness of DSP plate	m
θ	Zenith angle between the normal vector of a surface and the vector to the sun.	rad
α_{mps}	Solar absorptivity of MPS	
α_{tsdsp}	Solar absorptivity of bottom surface of DSP	
α_{bsdsp}	Solar absorptivity of bottom surface of DSP	
ε_{mps}	Emissivity of MPS	
ε_{tsdsp}	Emissivity of top surface of DSP	
ε_{bsdsp}	Emissivity of bottom surface of DSP	
σ	Stefan-Boltzmann constant, 5.67×10^{-8} W/(m^2K^4)	
ρ_c	Filling factor	
n_c	Solar cell efficiency	
MPS	Main part of satellite	
DSP	Deployable solar panel of satellite	